

Random walks near Rokhsar-Kivelson points

Olav F. Syljuåsen
 NORDITA, Blegdamsvej 17,
 DK-2100 Copenhagen Ø, Denmark
 sylju@nordita.dk

There is a class of quantum Hamiltonians known as Rokhsar-Kivelson(RK)-Hamiltonians for which static ground state properties can be obtained by evaluating thermal expectation values for classical models. The ground state of an RK-Hamiltonian is known explicitly, and its dynamical properties can be obtained by performing a classical Monte Carlo simulation. We discuss the details of a Diffusion Monte Carlo method that is a good tool for studying statics and dynamics of *perturbed* RK-Hamiltonians without time discretization errors. As a general result we point out that the relation between the quantum dynamics and classical Monte Carlo simulations for RK-Hamiltonians follows from the known fact that the imaginary-time evolution operator that describes optimal importance sampling, in which the exact ground state is used as guiding function, is Markovian. Thus quantum dynamics can be studied by a classical Monte Carlo simulation for any Hamiltonian that is free of the sign problem provided its ground state is known explicitly.

INTRODUCTION

Microscopic models that describe electronic behavior of materials are seldom exactly solvable. Nevertheless it is often found that lots of insight can be gained by studying a solvable model that resembles the accurate microscopic model in question. A typical approach is to neglect certain couplings in the accurate microscopic model in order to obtain a solvable model. This brings up the question of how important the neglected couplings are. One way of finding out is to simulate the accurate model numerically and compare to the results of the solvable model. If the results are sufficiently similar one can, with reasonable confidence, claim to understand the physical behavior using insights gotten from the solvable model.

The number of exactly solvable models are however relatively small. They tend to be either models of non-interacting particles, like free fermions, or non-trivial, but one-dimensional. Fortunately understanding and insight isn't necessarily tied to exactly solvable models. Models that can be fully or partially mapped onto other well-known models are also useful as older established results can be recycled.

There is a class of quantum models for which static ground state properties can be calculated by evaluating thermal expectation values of a corresponding *classical* model having the *same* number of space dimensions. This is a tremendous simplification as much are known about classical statistical mechanics models.

The most well-known of these quantum models is the quantum dimer model(QDM) at a special point in parameter space; the Rokhsar-Kivelson(RK) point[1]. There are also many other models with this property[2, 3, 4] with Hamiltonians known as (generalized) RK-Hamiltonians. Beside static properties it is also possible to obtain information about excited states and dynamical properties for RK-Hamiltonians, although in a rather unorthodox way. Henley[5] showed that dynamical cor-

relation functions at the RK-point can be gotten by performing a continuous-time Monte Carlo simulation of the classical model using appropriate Monte Carlo dynamics, and interpreting time- correlation functions of the classical simulation as imaginary-time correlation functions of the quantum system. This observation was recently utilized in Ref. [6] to determine excitations of the quantum dimer model on the triangular lattice at the RK-point. The observation that quantum dynamics can be gotten from classical Monte Carlo simulations is however not peculiar to RK-Hamiltonians. It is far more general, but requires knowledge of the *exact* ground state wave function. This was recently pointed out in Ref. [4], but follows also, as will be explained here, as a consequence using importance sampling with an optimal guiding function in Quantum Monte Carlo.

Assuming that the physics at the RK-point is understood or at least that it can be calculated relatively easily, it is interesting to ask if the same physics also holds away from the RK-point. An obvious approach to attempt answering this is to perform a finite-temperature path-integral Monte Carlo simulation of the full quantum model. This is more complicated than performing a classical Monte Carlo simulation at the RK-point, but can be carried out for most quantum models provided the temperature is high enough. This approach was followed by Moessner and Sondhi in order to show that the spin liquid state existing at the RK-point of the QDM on the triangular lattice also extends to other values of the parameters[7]. However it is difficult to push these methods to low temperatures. The non-local update techniques usually employed to speed up quantum Monte Carlo simulations such as loops[8], worms[9] or directed-loops[10] are not easily applicable to the quantum dimer model as the configurations on each time-slice are heavily constrained. The directed-loop method have however been used to study the classical dimer model, for which very impressive system sizes can be studied

effectively[11]. On the other hand the special Monte Carlo dynamics implied by the non-local moves doesn't correspond to the dynamics of the quantum dimer model at the RK-point.

In this review we will discuss another Monte Carlo technique which is an excellent tool to study models in the vicinity of RK-Hamiltonians at zero temperature. This technique, which is a continuous-time formulation of the well known Diffusion Monte Carlo(DMC) technique, becomes equivalent to a continuous-time classical Monte Carlo method for RK-Hamiltonians. In fact, as is true for any DMC method, it becomes equivalent to a classical Monte Carlo method whenever it is used in conjunction with importance sampling that employs the exact ground state wave function as guiding function.

We concentrate on systems close to RK-points here. As is well known with DMC-methods the quality of the results depend to a large extent on the quality of the guiding function. The advantage of being close to a RK-point is that the ground state wave function is known exactly at the RK-point and can be used as good approximate guiding function in its vicinity.

This review is divided into two main parts. In Sec. the numerical method is discussed in details. Particular emphasis is put on how to extract observables reliably. In Sec. the application of the method to perturbed RK-Hamiltonians is discussed, and results pertaining to the quantum dimer model on a square lattice are given.

QUANTUM MONTE CARLO

There are two main branches of Quantum Monte Carlo methods. The first type of methods uses a stochastic process to sample the finite temperature quantum partition function and extract observables from this. The main challenge using these methods is to engineer efficient updates as the objects, or variables, in the partition function are extended objects, or paths, as follows from the path integral formulation of quantum mechanics. A big step forward in finding efficient update schemes has been achieved using avatars of the Swendsen-Wang[12] cluster update, so called loop[8], worm[9] or directed-loop[10] updates. These Monte Carlo methods are exact in the sense that they have no systematic bias of any sort, they are easily formulated in continuous-time, and are easily programmable. A drawback, but also a source of flexibility, is the different ways one can construct these non-local updates. This needs to be reconsidered for all models in question, although it can be automated to a great extent and rules of thumb for how to choose good rules exists[13, 14]. The finite-temperature methods are most efficient at high temperatures, and the zero temperature behavior is only obtained asymptotically by performing simulations at decreasingly lower temperatures.

The other branch of Monte Carlo methods use stochas-

ticity to simulate the outcome of (repeated) matrix multiplications. This general class of methods is known as Projector Monte Carlo(PMC), -repeated multiplications of the same matrix projects out the eigenstate with the highest eigenvalue. For quantum systems one is interested in the *lowest* eigenvalue of the Hamiltonian. Thus in Green function Monte Carlo which is a particular projector Monte Carlo technique the iterated matrix is the inverse of the Hamiltonian. Another method, DMC, uses the matrix $\exp(-H\tau)$ where H is the Hamiltonian and τ is imaginary-time.

For long times, or equivalently many matrix multiplications, any initial state with some overlap with the true ground state will sample the components of the ground state wave function and ground state observables can be obtained. Moreover because DMC evolves the wave function identically to the imaginary-time evolution quantum dynamic observables can be obtained easily from the evolution of the state.

PMC techniques complement the finite-temperature techniques because they are genuine zero-temperature methods, -no extrapolations to zero temperature are necessary. They are also excellent at finding the ground state energy in different sectors of conserved quantum numbers, something which generally is difficult with the methods that work in the grand-canonical ensemble. Moreover no ingenuity in finding efficient updates is needed as everything is directly dictated by the Hamiltonian itself.

The evolution matrix in DMC is in general not a Markovian matrix. Thus DMC cannot be directly interpreted as a classical Monte Carlo method. The standard way[15] to cope with the lack of probability conservation is to include additional branching processes. Unfortunately these have a tendency to make simulations unstable and some feedback control is needed. This feedback results in a systematic bias[16] to the observables which can be removed by reweighting the simulation at the expense of additional statistical errors.

It is often stated repeatedly in the literature that DMC cannot be formulated in continuous (imaginary) time, and that repeated runs with decreasingly smaller time-intervals must be performed in order to quantify the error induced by a finite time-step. However the construction and implementation of a continuous-time formulation of DMC is straight-forward for lattice models[17], a fact we aim to explain in the next section. Other lattice PMC techniques[18] using different operators to project onto the ground state, such as for instance $1 - (H - E_0)\tau$, are also free of time-discretization errors. However these methods do not have the advantage, as do DMC, that quantum dynamics can be obtained easily. For another newly developed continuous-time Monte Carlo method, see Ref. [19].

Continuous-time Diffusion Monte Carlo algorithm

The basic idea behind DMC is to simulate the power method stochastically. The power method uses repeated matrix multiplications to project out the eigenstate having the largest eigenvalue. In DMC the imaginary-time evolution operator projects out the ground state of the Hamiltonian. Specifically

$$e^{-(H-E_0)\tau}|x_I\rangle \xrightarrow{\tau \rightarrow \infty} C_{x_I}|\psi_0\rangle \quad (1)$$

where H is the Hamiltonian, E_0 is the ground state energy and $|x_I\rangle$ is an arbitrary initial state having overlap $C_{x_I} = \langle \psi_0 | x_I \rangle$ with the ground state $|\psi_0\rangle$.

We will now explain how the multiplication by $e^{-(H-E_0)\tau}$ is carried out in continuous-time, that is without discretizing τ . Consider an N -state system with Hamiltonian matrix elements: $H_{ij} = \langle i | H | j \rangle$, where $i, j = \{1, 2, \dots, N\}$. For this N -state system an instance of the (unnormalized) wave function is described by an N -dimensional vector having non-negative integer entries

$$|\psi\rangle = \begin{pmatrix} M_1 \\ \vdots \\ M_N \end{pmatrix}. \quad (2)$$

This integer-valued vector represents $M = M_1 + M_2 + \dots + M_N$ replicas or copies of the system, where M_1 of them are in state number 1, M_2 are in state 2, etc.. For big systems the dimension of the vector is huge. With a finite number of replicas it will be very sparse and it is better to keep track of the state of each replica than writing down the vector explicitly. The requirement that the number of replicas in a given state is non-negative is rather restrictive, and is equivalent to the requirement that there is no sign problem. We will restrict ourself to these cases.

In order to build up the continuous-time formulation we will consider the evolution for an infinitesimal time step and then explain how to piece together (infinitely) many of these time steps in one shot. The action of the time evolution operator for an infinitesimal time step $d\tau$ on an instance of the state is

$$\begin{pmatrix} M'_1 \\ M'_2 \\ \vdots \\ M'_N \end{pmatrix} = \begin{pmatrix} D_{11} & -H_{12}d\tau & \cdots & -H_{1N}d\tau \\ -H_{21}d\tau & D_{22} & \cdots & -H_{2N}d\tau \\ \vdots & \vdots & & \vdots \\ -H_{N1}d\tau & -H_{N2}d\tau & \cdots & D_{NN} \end{pmatrix} \begin{pmatrix} M_1 \\ M_2 \\ \vdots \\ M_N \end{pmatrix} \quad (3)$$

where the diagonal elements are $D_{ii} \equiv 1 + (E_R - H_{ii})d\tau$. Note that the ground state energy, E_0 , is not known at the outset of the simulation. Therefore an estimator of the ground state energy known as the reference energy E_R is introduced and used instead. During the course of the simulation this reference energy will be adjusted and can be used to extract the ground state energy. One

should note that a time varying E_R causes the evolved wave function to deviate from the ground state wave function[16]. This can be repaired by re-weighting the simulation as will be discussed in Sec. .

We will now formulate a stochastic process that on average yields the evolution equation, Eq. (3). In the time interval $d\tau$ a replica in state $|i\rangle$ can undergo one out of four different processes with associated probabilities:

- “Transition”, change state to $|j\rangle$, $j \neq i$, probability $P_{Tj}(i)$.
- “Die”, that is $M_i \rightarrow M_i - 1$, probability $P_D(i)$.
- “Replicate”, that is $M_i \rightarrow M_i + 1$, probability $P_R(i)$.
- “Stay”, stay unchanged in state $|i\rangle$, probability $P_S(i)$.

The “Die” and “Replicate” processes are known as *branching* processes. As these are *all* possibilities, probability conservation implies

$$P_{Tj}(i) + P_D(i) + P_R(i) + P_S(i) = 1, \quad (4)$$

and must hold for all states $i = 1, \dots, N$.

The task of identifying the probabilities with matrix elements of the Hamiltonian is easy. Because the off-diagonal matrix element H_{ji} is the only one responsible for transition between state i and j it is clear that

$$P_{Tj}(i) = -H_{ji}d\tau \quad (5)$$

where $j \neq i$. In order to avoid the sign problem off-diagonal matrix elements are restricted to be negative.

The increase in the number of replicas in state $|i\rangle$ from processes acting on replicas in state $|i\rangle$ is

$$M'_i - M_i = \left[P_R(i) - P_D(i) - \sum_{j \neq i} P_{Tj}(i) \right] M_i. \quad (6)$$

This implies when comparing to the diagonal elements of Eq. (3) and using Eq. (5) that

$$P_D(i) - P_R(i) = \left(H_{ii} - E_R + \sum_{j \neq i} H_{ji} \right) d\tau. \quad (7)$$

The right hand side of the above takes either a positive or a negative value. In order to reduce the fluctuations in the replica numbers as much as possible $P_R = 0$ is chosen whenever this value is positive and $P_D = 0$ when it is negative. This choice implies that P_D and P_R are of the order $d\tau$ as also holds for P_T . The probability conservation equation Eq. (4) then implies

$$P_S(i) = 1 - \left(|H_{ii} - E_R + \sum_{j \neq i} H_{ji}| - \sum_{j \neq i} H_{ji} \right) d\tau, \quad (8)$$

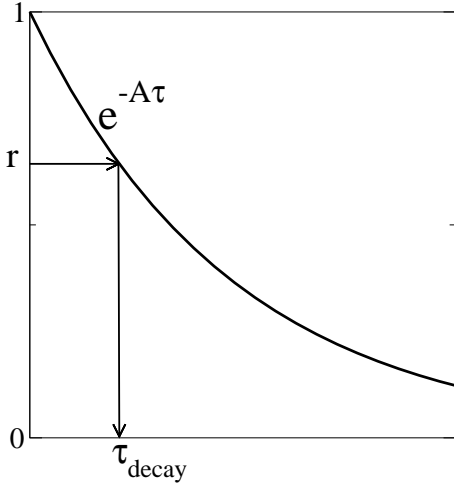


FIG. 1: Selecting decay times according to the exponential distribution with decay constant A . Drawing a random number r , the decay time τ_{decay} is selected as $\tau_{\text{decay}} = \frac{1}{-A} \ln(r)$.

which is of the order unity.

We are now at the stage where we wish to patch together many infinitesimal time steps. From the fact that P_S is of the order unity and all other processes are of the order $d\tau$ it follows that for most (infinitesimal) time intervals nothing happens to a replica. The process can thus be modeled like the radioactive decay problem, although with several different decay channels: “Transition”, “Die”, and “Replicate”. The “Transition” channel is further divided into possibly as many as $(N - 1)$ different channels corresponding to different non-zero values of H_{ji} . This observation has been used previously to construct continuous-time algorithms for finite-temperature quantum Monte Carlo methods [20].

It follows that the imaginary-time evolution of one replica can be simulated by generating exponentially distributed decay times with decay constant $A = |H_{ii} - E_R + \sum_{j \neq i} H_{ji}| - \sum_{j \neq i} H_{ji}$, see Fig. 1.

Having obtained the decay time, the type of decay is determined stochastically proportional to the respective probabilities P_T , P_D and P_R , which are all of the same order $d\tau$.

Practical implementation

Although the method is formulated in continuous-time it is convenient to use discrete control times τ_c^i at regularly spaced time-intervals $\Delta\tau$ as times where measurements are recorded and population control are being performed.

In an actual simulation each replica contains information about the state of the system as well as a “clock” indicating the starting time for the next evolution. The

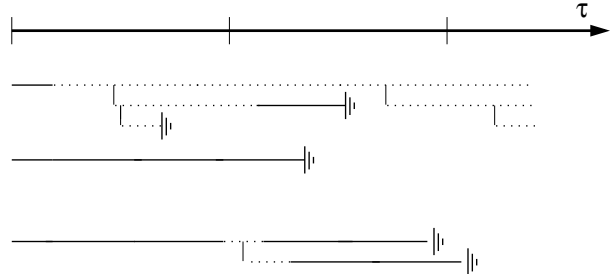


FIG. 2: Illustration of a possible evolution for a 2-state system. The top line is the imaginary-time axis, on which control times are indicated by vertical bars. Initially there are three replicas, all in state 1 labeled by solid lines. As time progresses replica 1 first “Transitions” to state 2 (dotted line), and then “Replicates”. Its replica also “Replicates”, but its copy “Dies” (the grounding symbol) almost immediately. Thus at the first control time the first replica has changed state and has divided into two. Nothing happens to the second replica up to the first control time, it just stays in the state 1. The third replica “Transitions” to state 2 just before the first control time. Having propagated all three initial replicas and their descendants up to the first control time, the population control procedure is performed before propagation up to the next control time starts.

replicas are ordered in a list. They all start in the same state and with their clock set to 0. Each replica in the list is subsequently evolved up to a control time τ_c , or until the replica dies in which case it is removed from the list. An evolution of a replica begins by generating a decay-time τ_d according to the exponential distribution. If $\tau_d > \tau_c$ the clock is set to τ_c and evolution of the next replica in the list starts. If however $\tau_d < \tau_c$, the clock is set to τ_d and a random number is drawn to select the decay type. If the decay type is “Transition” the state of the replica changes, if it is “Die” the replica is removed from the list, and finally the decay-type “Replicate” causes a copy of the replica with clock set to τ_d to be inserted at the end of the list. As long as the replica is not dead the evolution continues by picking a new decay time until τ_c is reached. When the last replica in the list has evolved up to τ_c , all replicas have the same clock-time, and measurements can be performed. The process is repeated by increasing τ_c and starting over from the beginning of the replica list. A graphical visualization of a possible evolution of replicas is shown in Fig. 2.

The control times are included in order to perform population control to avoid an explosion/implosion in the number of replicas. Population control is achieved by changing the value of the reference energy E_R so as to maintain a roughly constant number of replicas. E_R is only adjusted at the control times and is kept constant in between. Specifically, with E_R^i denoting the reference energy just *after* control time τ_c^i , which is the same value as just before the next control time τ_c^{i+1} , a possible choice

for population control is

$$E_R^i = \overline{E_R} + \frac{1}{\Delta\tau} \ln \left(\frac{N_0}{N_i} \right) \quad (9)$$

where N_i is the total number of replicas at τ_c^i and N_0 is the total number of replicas at the beginning of the simulation. $\overline{E_R}$ denotes the average value of E_R for all control time points up to τ_c^i . Thus when the number of replicas decreases below N_0 the reference energy is raised which will tend to increase the replication process, thereby increasing the replica population.

Observables

The measurement of observables in DMC requires some care[21]. There are two issues which need to be addressed. First one must get rid of the dependence on the choice of initial and final wave function. Then one must be careful about getting rid of the bias introduced by the population control procedure. Lets first explain how to get rid of the dependence on the initial and final wave functions. This is known as the forward- or future-walking method[22].

When the initial wave function is a particular basis state $|x_I\rangle$ the power method yields

$$e^{-H\tau}|x_I\rangle \xrightarrow{\tau \rightarrow \infty} C_{x_I}|\psi_0\rangle \quad (10)$$

where the overlap $C_{x_I} = \langle x_I|\psi_0\rangle$. For simplicity in notation we have absorbed the reference energy into the Hamiltonian in this section. The projection can of course also be carried out for a wave function which is the superposition (with unit coefficients) of all orthonormal basis states $|1\rangle \equiv \sum_x |x\rangle$

$$e^{-H\tau}|1\rangle \xrightarrow{\tau \rightarrow \infty} C_1|\psi_0\rangle. \quad (11)$$

This can be converted into an evolution of the dual state

$$\langle 1|e^{-H\tau} \xrightarrow{\tau \rightarrow \infty} \langle \psi_0|C_1. \quad (12)$$

Note that the overlaps are all assumed to be real and positive (in accordance with the restriction of having no sign problem).

In DMC the matrix evolution $e^{-H\tau}|x_I\rangle$ is replaced by a stochastic process

$$e^{-H\tau}|x_I\rangle = \sum_x P(x, \tau; x_I, 0)|x\rangle \quad (13)$$

where $P(x, \tau; x_I, 0)$ is the probability of finding the evolved state in the basis state $|x\rangle$ at time τ provided it was in state $|x_I\rangle$ at time zero. The stationary distribution of this evolution is proportional to the ground state.

It follows that the following can be used as an estimator of the ground state

$$\begin{aligned} |\psi_0\rangle &\xrightarrow{N_\tau \rightarrow \infty} \frac{1}{C_{x_I}N_\tau} \sum_\tau |\psi_\tau\rangle \\ &= \frac{1}{C_{x_I}N_\tau} \sum_\tau \sum_x P(x, \tau; x_I, 0)|x\rangle \end{aligned} \quad (14)$$

where the sum over different values of τ contains N_τ terms and the first τ -value is taken after an initial equilibration value τ_e .

Using these relations one can obtain an expression for the ground-state matrix element of the observable described by the operator \mathcal{O}

$$\langle \psi_0|\mathcal{O}|\psi_0\rangle \xrightarrow{\tau', N_\tau \rightarrow \infty} \alpha \sum_\tau \langle 1|e^{-H\tau'}\mathcal{O}|x\rangle P(x, \tau; x_I, 0) \quad (15)$$

as well as for the norm of the ground state

$$\langle \psi_0|\psi_0\rangle \xrightarrow{\tau', N_\tau \rightarrow \infty} \alpha \sum_\tau \langle 1|e^{-H\tau'}|x\rangle P(x, \tau; x_I, 0). \quad (16)$$

To shorten notation we have collected the overlap coefficients and the number of measurements into a single constant $\alpha = 1/(C_{x_I}C_1N_\tau)$. The overlap coefficients cancel when considering the ratio

$$\langle \mathcal{O} \rangle = \frac{\langle \psi_0|\mathcal{O}|\psi_0\rangle}{\langle \psi_0|\psi_0\rangle}. \quad (17)$$

Diagonal observables

Lets now specialize to the case where the observable \mathcal{O} is a time-independent observable diagonal in the basis set $\{|x\rangle\}$. Then the ground state matrix element is

$$\begin{aligned} \langle \psi_0|\mathcal{O}|\psi_0\rangle &= \alpha \sum_\tau \sum_{x,x'} \langle 1|x'\rangle \langle x'|e^{-H\tau'}\mathcal{O}|x\rangle P(x, \tau; x_I, 0) \\ &= \alpha \sum_\tau \sum_{x,x'} \langle 1|x'\rangle P(x', \tau + \tau'; x, \tau) \mathcal{O}_x P(x, \tau; x_I, 0) \\ &= \alpha \sum_\tau \sum_{x,x'} P(x', \tau + \tau'; x, \tau) \mathcal{O}_x P(x, \tau; x_I, 0) \end{aligned} \quad (18)$$

where we have used $\langle 1| \equiv \sum_{x''} \langle x''|$, orthonormality of the set of basis states and the eigenvalue relation $\mathcal{O}|x\rangle = |x\rangle \mathcal{O}_x$. Similarly the norm is

$$\langle \psi_0|\psi_0\rangle = \alpha \sum_\tau \sum_{x'} P(x', \tau + \tau'; x_I, 0) \quad (19)$$

In both these expressions the limits $\tau, \tau' \rightarrow \infty$ are implied. This limit can of course not be achieved in practice so instead one evaluates the right hand sides with large values of τ and τ' .

Starting with typically thousands of replicas in the same initial state $|x_I\rangle$ the probability $P(x, \tau; x_I, 0)$ is proportional to the number of replicas in state $|x\rangle$ at time τ . Thus the denominator is simply the total number of replicas at time $\tau + \tau'$. The numerator is a bit trickier in that one counts the replicas at time $\tau + \tau'$ but with each replica weighted by the value of the observable at time τ . To implement this in practice it is convenient to let each replica keep track of its history of observation values. This list must at least be of the length τ' . Alternatively one could let each replica keep a history of its configurations, but this is quite memory-consuming, and it is better to concentrate on a few observables and their histories. The history list is such that whenever a walker replicates, the history list is also replicated such that the new walker inherits the same history as the original walker.

The measurements must be performed at identical times for all replicas. One way of doing this is to measure the observable at the control times and store the result in the history list for each replica. One can also pick the measurement point to be at an arbitrary time in the time interval between replicas, instead of at precisely the control time itself. In fact, one can take the average of the observable over all time points in the interval, so as to get the maximum information available. This is quite easy to implement as the observable only changes value when a decay of the “Transition” type happens. As the times of decays are known it is quite easy to compute the time-weighted average of the observable for the interval between control times. For instance, assuming that there is just one decay at τ_d changing the observable from \mathcal{O}_1 to \mathcal{O}_2 , the average value accumulated at the control time τ_c^i is then $(\mathcal{O}_1(\tau_d - \tau_c^{i-1}) + \mathcal{O}_2(\tau_c^i - \tau_d)) / (\Delta\tau)$. This average value is then stored in the replica’s history list of measurements.

Off-diagonal observables

It is slightly more complicated to measure off-diagonal static (time-independent) observables than diagonal observables as there are no ways to insert off-diagonal operators without disturbing the configurations. The trick usually employed, which only works when the off-diagonal operator is a term in the Hamiltonian is best appreciated by visualizing the stochastic process as divided into small discrete time steps. That is

$$P(x, \tau; x_I, 0) = P(x, \tau; x_{n-1}, \tau_{n-1}) \dots P(x_2, \tau_2; x_1, \tau_1) P(x_1, \tau_1; x_I, 0) \quad (20)$$

This discretization is never used in practice, it is used here merely for explaining the measurement procedure. In the limit of infinitesimal time intervals the processes involving changes of states are related to off-diagonal matrix elements of the Hamiltonian $P(y, \tau + d\tau; x, \tau) =$

$-\langle y|H|x\rangle d\tau$, see Eq. (5). The matrix element of the off-diagonal operator can then be written

$$\langle \psi_0 | \mathcal{O} | \psi_0 \rangle = \sum_{x, x', x''} P(x', \tau' + \tau; x'' \tau) \langle x'' | \mathcal{O} | x \rangle \times P(x, \tau - d\tau; x_I, 0) \quad (21)$$

Note the “hole” introduced, there is nothing between $\tau - d\tau$ and τ . There is nothing wrong with having such a hole as the probabilities are invariant under time translations. Thus we can think of the left-most factor as being time-translated by an amount $d\tau$. Multiplying by

$$1 = \frac{P_{\mathcal{O}}(x'', \tau; x, \tau - d\tau)}{-\langle x'' | H_{\mathcal{O}} | x \rangle d\tau} \quad (22)$$

one gets

$$\langle \psi_0 | \mathcal{O} | \psi_0 \rangle = \sum_{x, x', x''} P(x', \tau' + \tau; x'', \tau) \times P_{\mathcal{O}}(x'', \tau; x, \tau - d\tau) P(x, \tau - d\tau; x_I, 0) \frac{\langle x'' | \mathcal{O} | x \rangle}{-\langle x'' | H_{\mathcal{O}} | x \rangle d\tau} \quad (23)$$

where the subscript \mathcal{O} indicates the transition described by the observable \mathcal{O} . There is nothing special about the time τ , other than it should be far from the starting and final time, thus we might take the average over many time intervals each of length $d\tau$ within a range of nearby control times (τ_c^{i-1}, τ_c^i) . Implementing this in practice amounts to counting the number of transitions corresponding to the off-diagonal operator in question within the time interval $\Delta\tau$ and multiplying this number by $\frac{\langle x'' | \mathcal{O} | x' \rangle}{-\langle x'' | H | x' \rangle \Delta\tau}$. This number is then stored as the measurement value at time τ_c^i in the history list, and the variables are accumulated in the same way as for diagonal observables using the forward-walking method where replicas are counted at $\tau + \tau'$ weighted by the measurement value at τ .

Dynamic observables

Dynamic observables can be recorded from the history list of measurement results for each replica. Dynamic correlation functions at times $\tau = m\Delta\tau$ significantly larger than the time interval between control times $\Delta\tau$ can simply be gotten by taking products of entries that differ by m slots in the history list. In order to measure the small time behavior using this approach $\Delta\tau$ should be made smaller. Of course, as the method is formulated in continuous-time, there is nothing in principle restricting the measurement times to discrete time points $m\Delta\tau$. At the expense of some extra book-keeping one can store and record observables at any time-separations.

Reweighting

The use of population control where the reference energy E_R is changed in order to keep the number of replicas approximately constant implies that the Monte Carlo procedure with population control is not sampling exactly the imaginary-time evolution of the wave function. Instead it is sampling an evolution with a time-dependent reference energy. Varying E_R according to the recipe described in Sec. the resulting wave function $\bar{\psi}$ will differ from the correct ground state wave function ψ by a prod-

uct of time-dependent factors[23]

$$\psi(\tau_i) = e^{-\sum_{k=0}^{i-1} (E_R^k - E_R^0) \Delta \tau} \bar{\psi}(\tau_i) \quad (24)$$

The subtraction of the constant E_R^0 is done in order to keep the exponential from overflowing.

The extra multiplicative factor coming from the time-varying E_R can be gotten rid of by multiplying by the exponential factor above, giving for a diagonal observable

$$\frac{\langle \psi_0 | \mathcal{O} | \psi_0 \rangle}{\langle \psi_0 | \psi_0 \rangle} = \frac{\sum_{x, x'} P(x', \tau_i; x, \tau) \mathcal{O}_x P(x, \tau; x_I, 0) e^{-\sum_{k=0}^{i-1} (E_R^k - E_R^0) \Delta \tau}}{\sum_x P(x', \tau_i; x_I, 0) e^{-\sum_{k=0}^{i-1} (E_R^k - E_R^0) \Delta \tau}} \quad (25)$$

Of course one cannot keep track of an infinite product of factors, and if one could, the fluctuations would be enormous, making it impossible to get accurate results[16]. However if the number of replicas isn't varying a lot, which can be achieved using importance sampling as described in the next section, the fluctuations need not be big[23].

In practice the observables are studied for different values of reweighting times. Typically one sees a clear bias without reweighting which is possible to avoid by taking longer reweighting times, however too long reweighting times gives added noise. Fortunately the bias vanishes usually before the noise gets big, thus there is a region where one can get accurate measurements, see Fig. 3.

Importance Sampling

It is known that importance sampling reduces statistical errors in DMC[24]. Importance sampling is achieved by sampling the product of the wave function times a guiding function instead of the wave function alone. The guiding function is chosen to be as close to the exact ground state as possible. Lets now show that branching can be avoided using importance sampling when the guiding function coincides with the exact ground state wave function. Consider the (infinitesimal time) evolution equation

$$\langle \sigma | \psi(\tau + d\tau) \rangle = \sum_{\sigma'} \langle \sigma | (1 + (E_R - H)d\tau) | \sigma' \rangle \langle \sigma' | \psi(\tau) \rangle \quad (26)$$

where $|\psi(\tau)\rangle$ labels the simulated instance of the wave function and $|\sigma\rangle$ denotes a basis state. Multiply by the time-independent guiding function $\langle \psi_g | \sigma \rangle$ and insert the

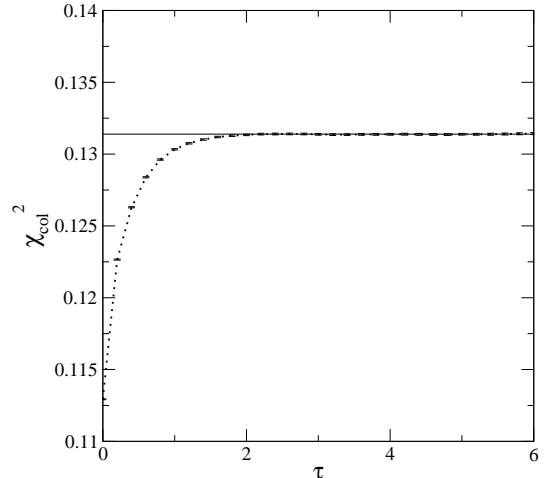


FIG. 3: Columnar order parameter χ_{col}^2 on a 4x4 lattice vs. reweighting times for the quantum dimer model at $V/J = 0.1$. $M = 1000$ replicas were used. The reweighting times are here defined using projections for τ steps to project onto the ground state and forward-walking for τ additional time steps. The line is the exact diagonalization result.

unity factor $\frac{\langle \psi_g | \sigma' \rangle}{\langle \psi_g | \sigma' \rangle}$

$$\begin{aligned} \langle \psi_g | \sigma \rangle \langle \sigma | \psi(\tau + d\tau) \rangle = \\ \langle \psi_g | \sigma \rangle \sum_{\sigma'} \langle \sigma | (1 + (E_R - H)d\tau) | \sigma' \rangle \frac{\langle \psi_g | \sigma' \rangle}{\langle \psi_g | \sigma' \rangle} \langle \sigma' | \psi(\tau) \rangle. \end{aligned} \quad (27)$$

As all eigenfunctions are real here, we do not distinguish between $\langle \psi | \sigma \rangle$ and $\langle \sigma | \psi \rangle$. The evolution matrix governing the evolution of the product $\langle \psi_g | \sigma \rangle \langle \sigma | \psi(\tau) \rangle$ is there-

fore

$$\langle \psi_g | \sigma \rangle \langle \sigma | (1 + (E_R - H)d\tau) | \sigma' \rangle \frac{1}{\langle \psi_g | \sigma' \rangle}. \quad (28)$$

Now take the case where the guiding function ψ_g coincides with the true ground state wave function. Then when we sum over columns of this matrix, that is \sum_{σ} and use the resolution of the identity, $1 = \sum_{\sigma} |\sigma\rangle\langle\sigma|$, we get

$$\begin{aligned} & \sum_{\sigma} \langle \psi_g | \sigma \rangle \langle \sigma | (1 + (E_R - H)d\tau) | \sigma' \rangle \frac{1}{\langle \psi_g | \sigma' \rangle} \\ &= 1 + \frac{\langle \psi_g | (E_R - E_0) d\tau | \sigma' \rangle}{\langle \psi_g | \sigma' \rangle} \end{aligned} \quad (29)$$

The last term vanishes provided $E_R = E_0$. The fact that each column sum to unity means that the matrix is Markovian. The evolution can then be simulated entirely without branching processes and is thus a *classical* Monte Carlo simulation in continuous-time.

The diagonal elements of the evolution matrix are not affected by the guiding function, while the off-diagonal ones are. This changes the transitions between the states. Basically the transition to a state is enhanced if the guiding function has a large value for that state. If the state it was coming from also corresponds to a large guiding function value, ψ_g^{-1} ensures that this is compensated for.

QUANTUM DIMER MODEL ON THE SQUARE LATTICE

We will now apply the continuous-time DMC method to perturbed RK-Hamiltonians taking the QDM on a square lattice as an example. The QDM was first proposed in the context of resonant valence bond (RVB) theories of high-Tc superconductivity[25]. In the RVB theory[26, 27] pairs of spins form singlets that are approximated by dimers in the QDM. The Hamiltonian is

$$H = -J \sum \left(|\uparrow\downarrow\rangle\langle\downarrow\uparrow| + H.c. \right) + V \sum \left(|\uparrow\uparrow\rangle\langle\uparrow\uparrow| + |\downarrow\downarrow\rangle\langle\downarrow\downarrow| \right) \quad (30)$$

where the summations are taken over all elementary plaquettes of the lattice. The basis states of the QDM consist of all possible dimer coverings of the lattice such that all sites are covered and no dimers overlap each other. The potential energy term V counts the number of plaquettes possessing parallel dimers and the J -term associates a kinetic energy to flips in the orientation of these parallel dimers. For this reason plaquettes possessing parallel dimers are named flipable plaquettes.

Rokhsar and Kivelson[1] realized that one could find the exact ground-state of this model at $J = V$. The

ground-state at this RK-point is simply the equal superposition of all basis states

$$|0\rangle = \frac{1}{\sqrt{N}} \sum_i |i\rangle \quad (31)$$

where $|i\rangle$ is a basis state describing a particular dimer covering of the lattice. N is the total number of basis states. Any ground-state expectation value of a time-independent operator diagonal in the basis states can then be evaluated as

$$\langle 0 | \mathcal{O} | 0 \rangle = \frac{1}{N} \sum_i \mathcal{O}_i \quad (32)$$

where the sum goes over all classical dimer covering states. The right hand side can be recognized as an expectation value in classical statistical mechanics taken at infinite temperature, where the classical partition function becomes $Z = N$.

The special property of the QDM at $V = J$ which makes the simple wave function Eq. (31) the ground state is the fact that the Hamiltonian can be written as a sum weighted by positive coefficients of positive semi-definite Hermitean operators acting on pairs of states, where each operator is proportional to its own square.

Eq. (32) describes a classical system at infinite temperature. The recipe for constructing finite-temperature RK-Hamiltonians was given in Ref. [4]. A quantum Hamiltonian of the form, which one can view as the general defining form of RK-Hamiltonians,

$$\begin{aligned} H_{RK} = & \sum_{\{s, s'\}} t_{s, s'} \left(e^{-K(E_{s'} - E_s)/2} |s\rangle\langle s| \right. \\ & \left. + e^{K(E_{s'} - E_s)/2} |s'\rangle\langle s'| - |s\rangle\langle s'| - |s'\rangle\langle s| \right) \end{aligned} \quad (33)$$

has the ground state

$$|\psi_0\rangle = \frac{1}{\sqrt{Z}} \sum_s e^{-KE_s/2} |s\rangle \quad (34)$$

with $E_0 = 0$, where $Z = \sum_s e^{-KE_s}$ and $t_{s, s'}$ res positive. It follows that the ground state expectation value of static quantities can be gotten by evaluating a classical thermal expectation value at inverse temperature K .

Quantum dynamics from classical Monte Carlo

In addition to the “classical” ground-state properties of RK-Hamiltonians it was pointed out by Henley that the quantum dynamics of the RK-Hamiltonian can be gotten by performing a classical Monte Carlo simulation with the appropriate dynamics[2, 5]. We want to show

that this relation between quantum dynamics and classical Monte Carlo is general. This was also recently discussed in Ref. [4]. Before doing so lets see what happens to the continuous-time DMC method for the QDM exactly at the RK-point as well as for the generalized RK-Hamiltonians in Eq. (33).

A state with f flipable plaquettes in the QDM has potential energy fV . Having f flipable plaquettes implies that f other states are accessible by one dimer flip, thus there is a kinetic energy $-fJ$ associated with this state. At the RK-point, $V = J$, the sum of potential and kinetic energy is thus zero. It follows from Eq. (7) that $P_D - P_R = 0$ provided E_R is set equal to the true ground state energy $E_0 = 0$. This holds for any basis state of the system. The fact that branching can be set to zero means that the DMC has been reduced to a classical Monte Carlo procedure.

For the generalized RK-Hamiltonians described in Eq. (33), the branching processes are not automatically zero. However branching can be avoided if one simulates the *product* of the wave function with the ground state wave function Eq. (34). According to Eq. (28) the Hamiltonian then changes effectively, $H \rightarrow \psi_g H \psi_g^{-1}$, meaning that diagonal terms are unchanged while off-diagonal terms, $H_{s's} \rightarrow e^{-K(E_{s'} - E_s)/2} H_{s's}$, where we have used the ground state of the RK-Hamiltonian Eq. (34) as guiding function. The amount of branching needed according to Eq. (7) becomes again

$$\begin{aligned} P_D(s) - P_R(s) &= \sum_{s' \neq s} t_{s,s'} e^{-K(E_{s'} - E_s)/2} \\ &\quad - \sum_{s' \neq s} t_{s,s'} e^{-K(E_{s'} - E_s)/2} \\ &= 0, \end{aligned} \quad (35)$$

provided $E_R = E_0 = 0$. Thus the DMC algorithm from which quantum dynamics can be extracted reduces to a pure *classical* Monte Carlo simulation when used in combination with importance sampling using the exact ground state as guiding function.

It is peculiar to note that in the quantum dimer model case the DMC method reduced to a classical Monte Carlo method without the explicit mentioning of a guiding function as was needed for the general RK-Hamiltonians. However, in fact the guiding function was used implicitly. This becomes clear when realizing that the ground-state Eq. (31) is the equal amplitude superposition of all basis states, thus $\psi_g(s)\psi_g^{-1}(s') = 1$ for all states s and s' . In other words the equal amplitude wave function is the default guiding function used in DMC when no other explicit guiding functions are specified. It corresponds simply to the multiplication by unity.

Having explained how optimal importance sampling leads to a classical Monte Carlo procedure for RK-Hamiltonians it should be clear that the underlying reason follows from the known importance sampling argu-

ment originally presented in Ref. [24] and restated in Sec. (); the operator governing the evolution of the wave function *times* the exact ground state wave function is a Markovian matrix. Thus quantum dynamics can be gotten from classical Monte Carlo simulations for *any* Hamiltonian that can be simulated with the DMC method provided the exact ground-state is explicitly known. The advantage of dealing with RK-Hamiltonians is the fact that their ground states and energies are known explicitly from the construction of the models.

Measurement results

Now turn to the physics of the QDM on the square lattice. For negative values of V it is favorable to have parallel arrangement of dimers around a plaquette. For positive V there is a potential energy cost to have such parallel arrangements, however the resonance term still favors parallel dimers. Thus it can be expected that the favorable dimer configurations maximize the number of parallel dimers also for positive V . In order to measure the dominance of parallel dimers we use the so called columnar order parameter which can be written as

$$\chi_{\text{col}}^2 = \frac{1}{4N^2} \left\langle \left(\sum n_{\text{H}}(\vec{r}) (-1)^{r_x} \right)^2 + \left(\sum n_{\text{V}}(\vec{r}) (-1)^{r_y} \right)^2 \right\rangle \quad (36)$$

where n_{H} (n_{V}) is the number of horizontal (vertical) dimers belonging to the plaquette at \vec{r} . \vec{r} is an integer-valued coordinate labeling the center of each plaquette on a lattice of size $N = L \times L$. The sums are to be taken over all plaquettes.

The columnar order parameter is a diagonal observable which does not commute with the Hamiltonian. It is therefore necessary to use the forward walking technique, which require reweighting.

Measuring the columnar order parameter for different system sizes at different values of V/J we obtain the results shown in Fig. 4 [17]. It is seen that the columnar order parameter remains finite for $V/J < 1$ and goes to zero at $V/J = 1$. These results are consistent with earlier results obtained using exact diagonalization[28, 29].

The columnar order parameter does not distinguish between columnar and plaquette phases, see Fig. 5.

To distinguish between these it is helpful to consider the order parameter[30]

$$\phi = \frac{1}{N} \sum (n_{\text{H}}(\vec{r}) - n_{\text{V}}(\vec{r})) \quad (37)$$

which is unity in the columnar phase and vanishes in the plaquette phase. A plot of $\langle \phi^2 \rangle$ as a function of V/J for different system sizes is found in Fig. 6. ϕ is seen to decrease as V/J increases. This is consistent with the plaquette phase being more favorable as one approaches the RK-point. In order to detect a phase transition we

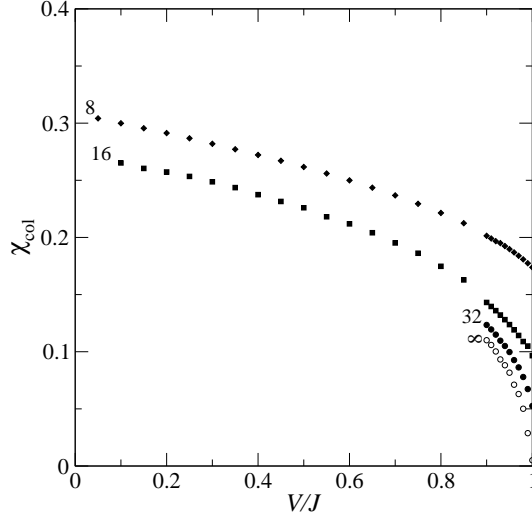


FIG. 4: Columnar order parameter χ_{col} vs. V/J . The different curves are for different linear system sizes $L = 8, 16, 32$ and the open symbols are (quadratic) extrapolations to $L = \infty$.

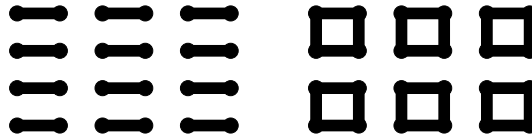


FIG. 5: Columnar phase (left) and plaquette phase (right). The presence of bonds indicates bigger probabilities for dimers than the absence of bonds.

measure $\langle \phi^2 \rangle$ and $\langle \phi^4 \rangle$ and form the Binder cumulant $g = 1 - \langle \phi^4 \rangle / (3\langle \phi^2 \rangle^2)$ for different system sizes. The cumulants for different system sizes should cross at the phase transition provided the scaling regime has been reached[31]. Using exact diagonalization the Binder cumulant was calculated for system sizes up to $L = 8$ using and the phase transition was estimated to happen at roughly $V/J = -0.2$ [29]. While we reproduce the exact diagonalization results for $L = 4, 6, 8$ we find that for larger L the crossing points moves towards larger values of V/J , see Fig. 7. It is rather difficult to pin down the exact location of the phase transition based on the crossing-points summarized in the inset of Fig. 7. However it is clear that the estimate $V/J = -0.2$ gotten from exact diagonalization studies is too low. Simulations on larger systems are needed in order to determine the accurate value.

Off-diagonal observables can also be measured. Consider the operator F measuring the energy associated with plaquette flips

$$F = \sum \left(|\mathbf{II}\rangle \langle \mathbf{II}| + \text{H.c.} \right) \quad (38)$$

where the sum is to be taken over all elementary pla-

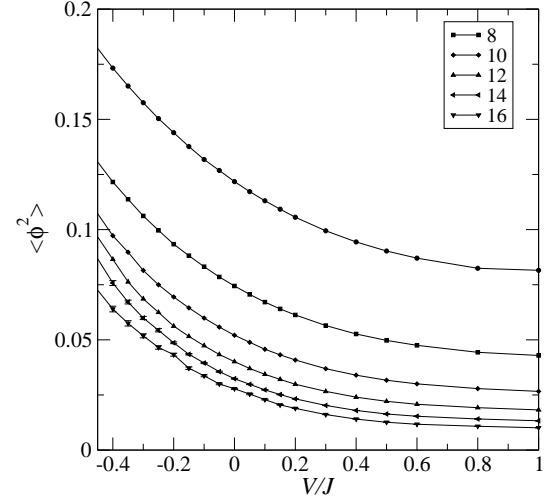


FIG. 6: The value of $\langle \phi^2 \rangle$ vs. V/J for different system sizes.

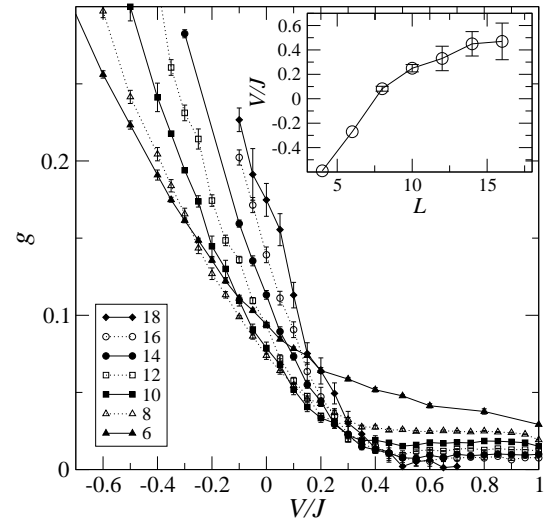


FIG. 7: Binder cumulant for the order parameter ϕ vs. V/J for different system sizes. The upper right inset is a blow-up of the region containing the crossings of the curves for the largest system sizes. The lower left inset shows the values of V/J at intersections between L and $L + 2$ curves.

quettes of the lattice. Figure 8 shows the ground-state expectation value of F measured directly using Eq. (23) (solid symbols) and indirectly measuring the potential energy which is a diagonal observable and subtracting that from the total energy (open symbols). It is evident that for parameters where the guiding function is not optimal the direct measurement of the offdiagonal observable is more noisy than the indirect measurement.

DMC has the advantage that imaginary-time correlation functions can be measured directly from the random walk. In Fig. 9 we show the equal bond dimer-dimer dynamic correlation function $D = \langle D_i(\tau)D_i(0) \rangle - \langle D_i \rangle^2$

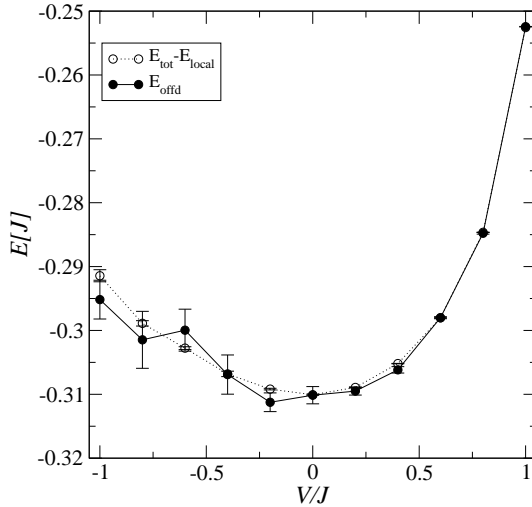


FIG. 8: Offdiagonal energy associated with plaquette flips vs. V/J for a 16×16 lattice. The solid symbols denote direct measurements of the offdiagonal terms and the open symbols are gotten from subtracting measurements of the potential energy (E_{local}) from the total energy (E_{tot}).

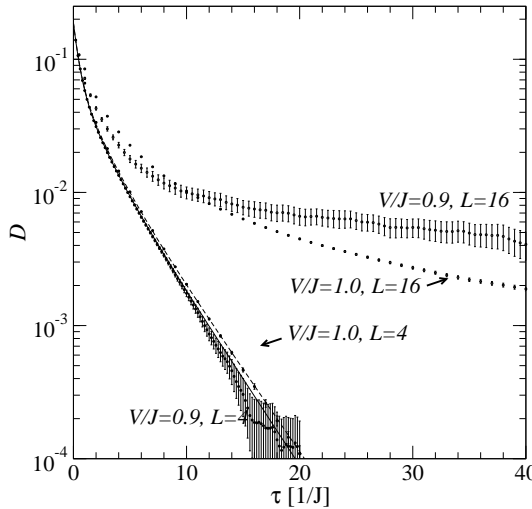


FIG. 9: semi-log plot of the equal bond dimer-dimer dynamic correlation function vs. imaginary time for different values of V/J . The curves are for a 16×16 lattice except for the two lowest curves which compares the Monte Carlo to exact diagonalization results on a 4×4 lattice.

(D_i is 1 if a dimer is present on bond i and 0 otherwise). The lowest two curves show the agreement with exact diagonalizations on a 4×4 -lattice (lines) for two values of V/J . Note the semi-log scale which “amplifies” the noise at small values of D . The upper two curves are for a 16×16 -lattice. By fitting the long time behavior to an exponential we find that the finite size gaps for the 16×16 -systems are $0.02 \pm 0.01J$ for $V/J = 0.9$ and $0.022 \pm 0.001J$ for $V/J = 1.0$.

CONCLUSIONS

We have explained in details a continuous-time formulation of the DMC method. The novelty of the method lies in its ability to output measurements of imaginary-time correlation functions without time discretization errors.

As any DMC method it performs best when used in combination with a good guiding function resembling the ground state wave function. Good guiding functions exist in the vicinity of RK-Hamiltonians, namely the explicitly known ground state of the RK-Hamiltonian itself. Thus the method performs well for perturbed RK-Hamiltonians.

In the case when the guiding function is equal to the exact ground state the DMC method becomes equal to a classical Monte Carlo procedure. Thus in these cases imaginary-time quantum correlation functions can essentially be obtained by classical Monte Carlo. This was pointed out in Ref. [5] for RK-Hamiltonians, but does in fact hold generally whenever the ground-state is known explicitly.

As examples of results that can be obtained using the continuous-time DMC we have calculated order parameters away from the RK-point in the QDM on the square lattice.

—

- [1] D. S. Rokhsar and S. A. Kivelson, *Phys. Rev. Lett.* **61**, 2376 (1988).
- [2] C. L. Henley, *J. Phys.: Condens. Matt.* **16**, S891 (2004).
- [3] E. Ardonne, P. Fendley and E. Fradkin, *Annals Phys.* **310**, 493 (2004).
- [4] C. Castelnovo, C. Chamon, C. Mudry, and P. Pujol, To be published in *Annals of Physics*, [arXiv: cond-mat/0502068].
- [5] C. L. Henley, *J. Stat. Phys.* **89**, 483 (1997).
- [6] D. A. Ivanov, *Phys. Rev. B* **70**, 094430 (2004).
- [7] R. Moessner and S. L. Sondhi, *Phys. Rev. Lett.* **86**, 1881 (2001).
- [8] H. G. Evertz, *Adv. Phys.* **52**, 1 (2003).
- [9] N. V. Prokof'ev, B. V. Svistunov, and I. S. Tupitsyn, *Pis'ma Zh. Eks. Teor. Fiz.* **64**, 853 (1996) [*JETP Lett.* **64**, 911 (1996)].
- [10] O. F. Syljuåsen and A. W. Sandvik, *Phys. Rev. E* **66**, 046701 (2002).
- [11] A. W. Sandvik, “Deconfinement and criticality in extended two-dimensional dimer models” [arXiv: cond-mat/0312097].
- [12] R. H. Swendsen and J.-S. Wang, *Phys. Rev. Lett.* **58**, 86 (1987).
- [13] O. F. Syljuåsen, *Phys. Rev. E* **67**, 046701 (2003).
- [14] F. Alet, S. Wessel, M. Troyer, “Generalized Directed Loop Method for Quantum Monte Carlo Simulations”, [arXiv: cond-mat/0308495].
- [15] M. D. Donsker and M. Kac, *J. Res. Natl. Bur. Stan.* **44**, 551 (1950).

- [16] J. H. Hetherington, in *Phys. Rev. A* **30**, 2713 (1984).
- [17] O. F. Syljuåsen, *Phys. Rev. B* **71**, R020401 (2005).
- [18] N. Trivedi and D. M. Ceperley, *Phys. Rev. A* **40**, 2737 (1989); *ibid.* **41**, 4552 (1990).
- [19] K. E. Schmidt, P. Niyaz, A. Vaught, and M. A. Lee, *Phys. Rev. E* **71**, 016707 (2005).
- [20] B. B. Beard and U.-J. Wiese, *Phys. Rev. Lett.* **77**, 5130 (1996).
- [21] M. P. Nightingale and C. J. Umrigar in *Advances in Chemical Physics* **105**, ed. D. M. Ferguson *et al.* (Wiley, New York, 1998), Chapter 4.
- [22] K.S. Liu, M.H. Kalos, and G.V. Chester, *Phys. Rev. A* **10**, 303 (1974).
- [23] C. J. Umrigar, M. P. Nightingale, and K. J. Runge, *J. Chem. Phys.* **99**, 2865 (1993).
- [24] M. H. Kalos, D. Levesque and L. Verlet, *Phys. Rev. A* **9**, 2178 (1974).
- [25] S. A. Kivelson, D. S. Rokhsar and J. P. Sethna, *Phys. Rev. B* **35**, R8865 (1987).
- [26] P. Fazekas and P. W. Anderson, *Philos. Mag.* **30**, 23 (1974).
- [27] P. W. Anderson, *Science* **235**, 1196 (1987).
- [28] S. Sachdev, *Phys. Rev. B* **40**, 5204 (1989).
- [29] P. W. Leung, K. C. Chiu and K. J. Runge, *Phys. Rev. B* **54**, 12938 (1996).
- [30] M. E. Zhitomirsky and K. Ueda, *Phys. Rev. B* **54**, 9007 (1996).
- [31] K. Binder, *Phys. Rev. Lett.* **47**, 693 (1981).